

SMALL ANGLE X-RAY SCATTERING
FROM THIN PLATES

by

RALPH WAYNE DELTENRE



B. S., Kansas State College
of Agriculture and Applied Science, 1955

—

A THESIS

submitted in partial fulfillment of the

requirements for the degree

MASTER OF SCIENCE

Department of Physics

KANSAS STATE COLLEGE
OF AGRICULTURE AND APPLIED SCIENCE

1956

L D
2668

T4
1956

D45

C.2

Documents

11

TABLE OF CONTENTS

INTRODUCTION	1
THEORY	4
General Considerations	4
Scattering from Infinitesimally Thin Circular Disc	10
Scattering from Circular Disc of Finite Thickness	13
Methods of Approximation	14
Refraction, Reflection Effects	17
EXPERIMENTAL APPARATUS	18
Collimation Geometry	18
Slit Construction	20
Scattering Chamber	22
Film Holder and Beam Stop	22
EXPERIMENTAL PROCEDURES	23
Exposure and Analysis of Films	23
Calibration	26
Sample Preparation	28
DISCUSSION OF RESULTS	31
CONCLUSIONS	37
SUGGESTIONS FOR FUTURE STUDIES	38
ACKNOWLEDGMENT	40
LITERATURE CITED	41

INTRODUCTION

The fundamental equation of x-ray diffraction, $\lambda = 2d \sin \theta$, indicates that for monochromatic radiation the scattering angle varies inversely with the lattice spacing. The order parameter usually associated with Bragg's law is included in d . In ordinary crystals the lattice spacing is the same order of magnitude as the wavelength of x-radiation and the scattering occurs through the angular region 0 to 90° . However, in the study of structures whose spacings are of the order of tens or hundreds of interatomic distances, the scattering angles will be quite small. Although this small angle scattering was observed and studied as early as 1925 (5), it was not until 1939 that Guinier (3) presented a theory which satisfactorily explained the observations.

When an x-ray beam impinges upon a material of constant electron density the electric field intensity is given by:

$$E \sim E_0 \int_v \rho e^{\frac{2\pi i}{\lambda} (\bar{s} - \bar{s}_0) \cdot \bar{r}} dv \quad (1)$$

where E is the electric field intensity of the incident beam, ρ is the electron density, λ is the wavelength of the incident x-ray beam, \bar{s} is a unit vector in the direction of the scattered beam, \bar{s}_0 is a unit vector in the direction of the incident beam, \bar{r} is the distance between two scattering centers, and dv is an element of volume of the scattering material.

It is the intensity of the scattered beam that is observed and this is proportional to the square of the electric field intensity. To obtain the intensity as a function of the scattering angle, equation (1) must be integrated over the volume of the particle which diffracts the x-ray beam. In the case of a spherical particle or a thin circular disc the solution of the integral in equation (1) involves a Bessel function. The Bessel function

varies with the same frequency as the exponential under the integral.

Any exponential of the form $e^{2\pi n i}$, where n is an integer, oscillates with a period of 2π . If the solution of the integral in equation (1) varies with the same period the condition must follow that

$$n = \frac{1}{\lambda} (\bar{s} - \bar{s}_0) \cdot \bar{r}$$

The integer, n , can be taken as one so that

$$\lambda = (\bar{s} - \bar{s}_0) \cdot \bar{r}$$

If 2θ is the scattering angle, then the magnitude of $(\bar{s} - \bar{s}_0)$ is $2 \sin \theta$ and

$$\lambda = 2 \sin \theta \cos \phi r$$

$$\text{or } \sin \theta = \frac{\lambda}{2 r \cos \phi} \quad (2)$$

where ϕ is the angle between $(\bar{s} - \bar{s}_0)$ and \bar{r} . For small angles $\sin \theta$ can be replaced by θ and equation (2) can be written as

$$\theta = \frac{\lambda}{2 r \cos \phi} \quad (2a)$$

Thus, the scattering angle varies inversely with the radius of the particle. If the radius of the particle is much larger than the wavelength of the incident radiation, the scattering angle will be small. If the particle is too large, however, the angle will be so small that the scattered radiation will be indistinguishable from the unscattered beam. On the other hand, if the particle is too small, the scattering angle will be large but the intensity will be spread out over such a large region that it would be hard to detect. Therefore, particles of a limited size range can be studied by small angle

scattering. This size range extends from 50 to 1000 Å for the radii of the particles.

Since the electric intensity is often an oscillating function, the intensity will vary and the intensity scattered from a particle of constant electron density will be a series of maxima within a few degrees of the incident beam. This same pattern will be observed if the beam is incident upon a group of particles of constant size and shape. The position of the various maxima can be used to determine the size of the particles. Most often the particles are not of constant size and the scattered intensity will no longer be a series of maxima and minima but rather a continuous scattering. In these cases it is the shape of the central maximum that gives the most information about the particle size.

For the case of spherical particles equation (1) has been solved giving

$$E \sim \frac{J_{\frac{1}{2}}(KR)}{(KR)^{\frac{1}{2}}}$$

and

$$I \sim \frac{J_{\frac{1}{2}}^2(KR)}{(KR)^3} \quad (3)$$

where $k = \frac{4\pi}{\lambda} \sin \theta$ and R is the average radius of the particles. This equation cannot be easily solved for R and so an approximate solution must be used. The best approximation was found to be a Gaussian function of the form:

$$I \sim e^{-\alpha^2 K^2 R^2}$$

By matching the areas under the Gaussian curve and the curve of equation (3) the value of α was found to be 0.221. In I can be plotted as a function

of k^2 and the radius R can then be found from the slope of this curve.

The purpose of this work was to find a method of determining the size parameters of non-spherical particles.

A good example of a non-spherical particle is kaolinite, a common soil clay mineral. The kaolinite particle is a pseudo hexagonal plate. Electron micrographs of the particles are shown in Plate I.

THEORY

General Considerations

The problem of determining the size parameters of non-spherical particles can best be attacked by first orienting the particles so that the axes of symmetry of each particle are in the same direction. The incident beam then sees each particle in the same orientation. The scattered intensity will depend not only upon the size and shape of the particles, but also upon their orientation with respect to the beam. By placing appropriate limits on the integral in equation (1), the scattered electric field intensity can be found as a function of size, shape and orientation. If the particles are not symmetric, they may be oriented with respect to the beam in three ways and three intensity equations can be found. Each equation will, in general, be a function of all three dimensions.

Equation (1) can be simplified by eliminating the vector relations in the exponential. The dot product can be expanded as

$$E = \rho \int e^{2\pi i (\vec{s} \cdot \vec{r} - \vec{s}' \cdot \vec{r}')} d\omega \quad (1a)$$

EXPLANATION OF PLATE I

Electron micrographs of kaolinite particles enlarged 30,600 times.

PLATE I

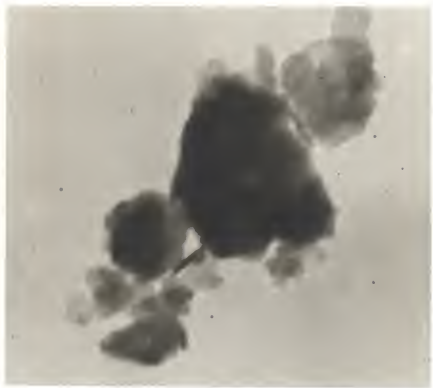


Fig. 1



Fig. 2

The dot products can be written in terms of scalar quantities giving

$$E = P \int_v e^{\frac{2\pi i}{\lambda} r [\cos(s, r) - \cos(s_0, r)]} dv \quad (1b)$$

since the magnitude of \vec{s} and \vec{s}_0 is unity.

The electric field is given here in electron units. This is found by dividing the actual electric field intensity by $\frac{E_0 e^2}{mc^2 R}$ where E_0 is the amplitude of the incident electric field, e and m are the charge and mass of the electron, respectively, c is the velocity of light, and R is the sample to detector distance.

With no loss of generality the direction of the incident beam, \vec{s}_0 , can be taken as the x axis and the scattering angle, 2θ can lie in the x,y plane as shown in Plate II, Fig. 1. The cosine terms can then be expanded into rectangular coordinates.

$$\cos(s, r) = \frac{x}{r}$$

$$\cos(s, r) = \cos(s, x) \cos(r, x) + \cos(s, y) \cos(r, y) + \cos(s, z) \cos(r, z)$$

since the cosine of the angle between any two lines in space is the sum of the products of the respective direction cosines. This equation further reduces to

$$\cos(s, r) = \frac{x}{r} \cos 2\theta + \frac{y}{r} \sin 2\theta$$

$$r [\cos(s, r) - \cos(s_0, r)] = x \cos 2\theta + y \sin 2\theta - x$$

$$= x (\cos 2\theta - 1) + y \sin 2\theta$$

EXPLANATION OF PLATE II

- Fig. 1. Scattering from two scattering centers.
- Fig. 2. Scattering with beam incident perpendicular to plane of particle.
- Fig. 3. Scattering with incident beam parallel to plane of particle, scattered beam perpendicular to plane of particle.
- Fig. 4. Scattering with incident beam parallel to plane of particle, scattered beam parallel to plane of particle.

PLATE II

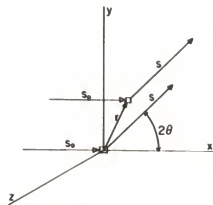


Fig. 1

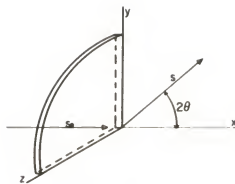


Fig. 2

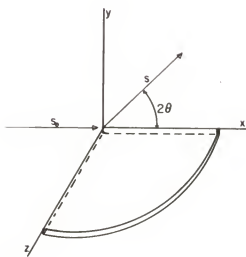


Fig. 3

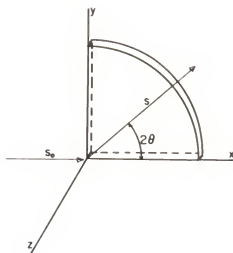


Fig. 4

Writing $dV = dx dy dz$, the electric field becomes

$$E = \rho \iiint e^{\frac{2\pi i}{\lambda} [x(\cos 2\theta - 1) + y \sin 2\theta]} dx dy dz$$

By making the substitution

$$k' = \frac{2\pi}{\lambda} \sin 2\theta$$

$$k'' = \frac{2\pi}{\lambda} (\cos 2\theta - 1)$$

the electric field intensity is further simplified:

$$E = \rho \iiint e^{ik''x + ik'y} dx dy dz \quad (4)$$

This is a general equation with the only restriction being that the electron density be constant over the region of integration.

Scattering from Infinitesimally Thin Circular Disc

The solutions of the three intensity equations are given in Plate III along with the intensity for the case of randomly oriented particles. To show how these were obtained equation (4) will be solved for the case of the beam striking the disc perpendicular to the plane of the disc as shown in Plate III, Fig. 2. In this case $x = 0$ and equation (4) becomes

$$E = 2\rho \iint_0^R e^{ik'y} dz dy \quad (5)$$

By simple integration

$$E = 2\rho \int_{-R}^R e^{ik'y} dy \quad (5a)$$

EXPLANATION OF PLATE III

Table showing intensity as a function of radius and thickness of particle and scattering angle for various orientations of the particles with respect to the incident beam. In these equations n is the number of electrons per unit volume, J is a Bessel function, R and T are the radii and thickness of the particles, respectively, 2θ is the scattering angle, and λ is the wavelength of the incident x-ray beam.

PLATE III

INTENSITY OF SCATTERING FROM FLAT DISCS

ORIENTATION	INFINITESIMALLY THIN	FINITE THICKNESS
RANDOM	$4n^2 \frac{J_1^2(KR)}{(KR)^2}$	
BEAM \perp PLATE	$4n^2 \frac{J_1^2(K'R)}{(K'R)^2}$	$4n^2 \frac{J_1^2(K'R) \sin^2(K''T/2)}{(K'R)^2 (K''T/2)^2}$
BEAM \parallel PLATE SCATTERING \parallel PLATE	$4n^2 \frac{J_1^2(KR)}{(KR)^2}$	$4n^2 \frac{J_1^2(KR)}{(KR)^2}$
BEAM \parallel PLATE SCATTERING \perp PLATE	$4n^2 \frac{J_1^2(K''R)}{(K''R)^2}$	$4n^2 \frac{J_1^2(K''R) \sin^2(K'T/2)}{(K''R)^2 (K'T/2)^2}$

 n = no. of electrons / particle R = radius of discs T = thickness

$$K = \frac{4\pi}{\lambda} \sin \theta$$

$$K' = \frac{2\pi}{\lambda} \sin 2\theta$$

$$K'' = \frac{2\pi}{\lambda} (\cos 2\theta - 1)$$

The solution of this integral can be found in Watson's Treatise on the Theory of Bessel Function. It is

$$E = 2\rho \frac{\pi R}{k'} J_1(k'R) \quad (5b)$$

The electron density $\rho = \frac{n}{\pi R^3}$ where n is the number of electrons per unit volume. Making the substitution equation (5a) becomes

$$E = 2n \frac{J_1(k'R)}{(k'R)} \quad (5c)$$

$$\text{and} \quad I = 4n^2 \frac{J_1^2(k'R)}{(k'R)^2} \quad (6)$$

Again, the constant terms in the intensity have been dropped for simplicity. The intensity equations for the other orientations are found in a similar manner.

Scattering from Circular Disc of Finite Thickness

If the thickness is denoted by T , equation (4) becomes, for the case of the beam incident perpendicular to the particle:

$$E = 2\rho \int_{-R}^R \int_0^{\sqrt{R^2-y^2}} e^{ik'y} dy dx \int_{-T_2}^{T_1} e^{ik''x} dx \quad (7)$$

The integral can be separated in this manner because the last part involves neither y nor z . The double integral over y and z is exactly the same as the one which was solved in the case of the infinitesimally thin disc. Using that result equation (5b) becomes

$$E = 2\rho \frac{\pi R}{k'} J_1(k'R) \int_{-Y_2}^{Y_2} e^{ik''x} dx \quad (7a)$$

By simple integration this becomes

$$E = 2\rho \frac{\pi R}{k'} J_1(k'R) \left[\frac{e^{ik''Y_2} - e^{-ik''Y_2}}{ik''} \right]$$

The quantity in the bracket is just $\frac{2}{k''} \sin(k''T/2)$ and

$$E = 2\rho \frac{\pi R}{k'} J_1(k'R) \frac{2}{k''} \sin(k''T/2) \quad (7b)$$

In this case ρ is $\frac{2\pi}{\pi R T}$: Making this substitution

$$E = 2n \frac{J_1(k'R)}{(k'R)} \frac{\sin(k''T/2)}{(k''T/2)} \quad (7c)$$

$$\text{and } I = 4n^2 \frac{J_1^2(k'R)}{(k'R)^2} \frac{\sin^2(k''T/2)}{(k''T/2)^2} \quad (8)$$

The intensity equations for the other orientations are given in Plate III. It should be noted that with the beam striking the edge of the plate and the scattering angle in the plane parallel to the particle as shown in Plate II, Fig. 4, the intensity is independent of the thickness of the particle.

Methods of Approximation

When the beam strikes a flat circular disc, such as a kaolinite particle, parallel to the plane of the particles and the scattered angle is in the same plane, the intensity is given by

$$I = \frac{4 J_1^2(KR)}{(KR)^2} \quad (9)$$

and, since k is a function of the scattering angle, the intensity is a function of both the particle radius and the scattering angle. The intensity and scattering angle can be measured and R must be given as a function of these two variables if its value is to be determined. Equation (9) cannot be easily solved to give R explicitly, so an approximation must be used. The best approximation has been found to be a Gaussian function of the form $e^{-\beta^2(KR)^2}$. To find the value of β the areas under both curves are set equal:

$$\int_0^\infty e^{-\beta^2(KR)^2} d(KR) = 4 \int_0^\infty \frac{J_1^2(KR)}{(KR)^2} d(KR) \quad (10)$$

The solution of the integral on the left side of equation (10) can be found in most tables of definite integrals and is equal to $\frac{\sqrt{\pi}}{2\beta}$. The solution of the right side of equation (10) is found in Watson's Treatise on the Theory of Bessel Functions. It is given as $\frac{4}{3\pi}$. From these values β was found to be 0.522, and β^2 is 0.272. With this substitution the intensity is approximated by

$$I = e^{-0.272(KR)^2}$$

Taking the natural log of both sides

$$\ln I = -0.272 K^2 R^2 \quad (11)$$

If $\ln I$ is plotted as a function of k^2 , a straight line will result for a uniform particle size with a slope of $-0.272R^2$ from which R can be obtained. If there are particles of more than one size present, several straight lines will be super-imposed. The tangent of the resulting curve can then be used to determine the range of R .

The thickness can be found in a similar manner. The intensity is approximated by

$$I = e^{-\frac{4\pi}{\lambda}(b^2x^2 + d^2y^2)}$$

If the beam is incident perpendicular to the plane of the particle, x and y are given by

$$x = \frac{4\pi}{\lambda} R \sin \theta \cos \theta$$

$$y = \frac{2\pi T}{\lambda} \sin^2 \theta$$

When the angles are small, these will become

$$x = \frac{4\pi}{\lambda} R \theta$$

$$y = \frac{2\pi T}{\lambda} \theta^2$$

The values of b and d were found to be 0.273 and 0.368 respectively. Making these substitutions

$$I = e^{-\frac{4\pi^2}{\lambda^2}(1.092R^2 + 0.361T^2\theta^2)\theta^2} \quad (12)$$

Taking the natural log of both sides

$$\ln I = - \frac{4\pi}{\lambda} (1.092 R^2 + 0.368 T^2 \theta^2) \theta^2$$

$$\text{or } \ln I = -k^2 (0.273 R^2 + 0.092 T^2 \theta^2) \quad (13)$$

If $\ln I$ is plotted as a function of k^2 the slope of the resulting curve will be $-(0.273 R^2 + 0.092 T^2 \theta^2)$. The slope is a linear function of θ with a slope of $0.092 T^2$. By plotting the slope of equation (13) as a function of θ^2 , the thickness can be obtained independently of the radius.

Refraction, Reflection Effects

When an x-ray beam impinges upon a group of large particles, the small angle diffraction scattering occurs at such small angles that the scattered intensity cannot be detected. Some scattering from larger particles has been observed, though (5). This scattering was clearly not due to diffraction scattering and was first explained by Von Hardroff (6) as due to refraction and total reflection of the x-ray beam by the particles.

Since the index of refraction for x-radiation is less than one, an x-ray beam striking a medium will be bent away from the normal to the surface. If the beam impinges upon a convex surface, such as a spherical particle, the beam will be bent away from the direction of the incident beam. When the beam strikes the second surface, or emerges from the particles, it is bent even further in the same direction. Thus, a beam striking a particle with convex surfaces will be diverged. At some point on the surface, the beam will be incident at such an angle with the normal to the surface that it will

be totally reflected.

The scattering due to refraction and reflection has been used to determine the particle sizes of spherical particles. The relations between refraction, reflection scattering and small angle diffraction scattering has been presented by Dragsdorff (2).

The radius of a spherical particle as given by Von Hardroff is

$$R = \frac{6VD\delta^2(\frac{1}{2} + \ln \frac{\gamma_0}{\gamma})}{\frac{\lambda^2}{8\pi^2 m} - \omega_0^2} \quad (14)$$

where V is the specific volume of the sample, D the thickness of the sample, δ is given by $1/\mu$, where μ is the index of refraction, m is the slope of the $\ln I$ vs. k^2 curve, and ω_0 is the width of the undeviated beam at half the maximum intensity.

EXPERIMENTAL APPARATUS

The experimental apparatus consisted primarily of an x-ray machine, a system of collimating slits, and a scattering chamber. Film was used as a detector and the scattering pictures were analyzed with a microdensitometer.

A copper target x-ray tube was used. The beam was monochromatized with a nickel filter so that radiation of a narrow band of wavelength, around 1.54 \AA , passed into the camera.

Collimation Geometry

The study of small angle x-ray scattering requires a beam of very small cross section and divergence. Since the scattering is through angles of less than three degrees, a beam of large cross section or divergence would

obscure most of the scattering. When slit collimation is used, this results in a beam of low intensity. It is essential then that the best geometrical conditions be obtained.

Two slits will define a beam but there may be some scattering by one or both of these slits. This is due to fluorescent scattering by the slit edges. It can be eliminated by placing a third slit between the second slit and the sample. The edges of the third slit should closely approach but not touch the primary beam. The primary beam will have a width, b , as determined by the first two slits, at the plane of the film. Although the scattering by the slit edges covers a large area, the third slit guards all but a small area of width, a . The width a is, of course, larger than b and the geometry is usually such that a is at least twice b . The collimation geometry depends upon the value chosen for b . The optimum value of b is found from the relation

$$b = \frac{s\lambda}{d_{max}}$$

where λ is the wavelength of radiation employed, d_{max} is the spacing of the largest structure to be studied, and s is the sample to film distance. Once these values have been chosen the conditions for optimum geometry have been given by Bolduan and Bear (1) as

$$r = \frac{b_p}{2 + b_p}$$

$$q = \frac{(2+b)b_p}{(2-b)b+2p}$$

$$v = \frac{2(s+t)[(2-b)b+2ap]p}{(2-b)b(b+2p)}$$

$$\omega = \frac{2(s+t)b_p}{(2-b)(b+2p)}$$

where p , r , and q are the widths of the first, second and third slits, respectively, v is the distance between the first two slits, w is the distance of the third slit from the second, and t is the distance from the

third slit to the sample.

The total distance, $v + w + s + t$, was determined by the space available and $v + w$ was determined by the length of the track on which the slits were mounted. The width, p , of the first slit is determined by the size of the focal spot of the x-ray tube. For the tube used the best value of p was found to be 0.1 mm. The other values used were: $b = 0.55$ mm., $a = 2b = 1.10$ mm., $v + w = 30.5$ cm., and $s + t = 42$ cm. Using these values in the equation given above, the other dimensions were found to be $r = 0.073$ mm., $q = 0.17$ mm., $v = 193$ mm., and $w = 112$ mm. The height of the beam in Bolduan and Bear's calculation is arbitrary. The beam height in the apparatus used in this work was restricted to 5 mm. at the sample.

Slit Construction

The apertures were made of lead plates approximately 2.5×3 c. and 4.5 mm. thick. The edges which defined the beam were beveled and mounted with the sharp edge facing the x-ray tube. This was done to eliminate, as much as possible, any reflection or diffraction by the slit edges.

The first slit was mounted directly on the x-ray tube. The width of the aperture was determined by brass shims placed between the lead plates. The lead plates were placed against the x-ray tube and held in place by a brass plate which was bolted to the tube. The brass plate had a hole in it a little larger than the window of the x-ray tube so that the brass did not obstruct the beam. Alignment was checked visually with a zinc sulfide screen. The height of the slit was 2.8 mm.

The second and third slits were identical in construction. The lead pieces were clamped in holders which were so made that both lead pieces would be moved to adjust the width of the slit. Each brass holder was then placed in another holder which was mounted on a track so that the position of each slit would be varied.

After the first slit was in position, the second slit was placed in position and adjusted to the proper width. This was done by closing each side of the slit until it touched the beam. A geiger counter placed in the path of the beam indicated when the lead touched the beam by a drop in the counting rate. The slit holder was then removed and the lead plates closed to the proper width under a microscope. To insure that the slit width would not change if the holder were accidentally bumped, brass shims of the same thickness as the slit width were placed between the lead plates at the outer edges so that they would not interfere with the beam. The slit was placed in the beam again and the alignment was checked visually with the zinc sulfide screen. The geiger counter was also used in checking the alignment and a final check was made photographically by exposing a film placed in the film holder in the scattering chamber. The height of both the second and third slits was 8 mm.

The same procedure was then followed with the third slit. After it was in place a brass frame was placed around the system and covered with lead. This contained all the scattering which did not pass through the slits to eliminate extraneous scattering into the room.

The height of the beam at the sample was limited by a lead plate mounted on the sample holder, directly in front of the sample. The beam passed symmetrically through a hole in the lead plate. The hole was 5 mm.

in diameter.

Scattering Chamber

The scattering chamber was an evacuated brass cylinder 36 cm. long and 10 cm. in diameter. A one inch hole drilled in one end was covered with a sheet of nickel which served as a window for the x-ray beam and also as the monochromating filter. The nickel was soldered to the brass to hold approximately a 30 micron vacuum. A track was placed along the bottom of the chamber to guide the beam stop and film holder. A brass plate was bolted to the rear of the chamber with a plastic gasket between the plate and chamber to hold the vacuum. The plate was easily removed and replaced to facilitate replacing the film holder.

The chamber was supported by three adjustable screws which were in turn mounted on a three inch iron box beam.

The sample was located on the outside of the scattering chamber, just in front of the nickel window. A mounting on the front of the chamber, just below the nickel window, held the sample holder. The sample could be changed easily without disturbing the collimator or scattering chamber.

Film Holder and Beam Stop

The film holder consisted of a circular brass plate covered on one side with black velvet. The plate was 9.7 cm. in diameter. The film was placed on the velvet and a brass ring covered with aluminum foil was placed over it and clamped to the brass plate. The brass ring fitted against the velvet making a light seal and the aluminum foil served as a window for the x-rays and as a light seal. A brass block was screwed to the lower edge of the

brass plate. A groove was made in both the plate and the block so that the film holder could be placed on the track in the scattering chamber. A set screw was put in the brass block so that it could be clamped to the track.

The beam stop was made by bending a square piece of thin copper sheet around a wire to form a U. The copper U was soldered to the wire and the U entirely filled with solder. This made a beam stop of width 1.5 mm. To hold the stop in place a brass ring similar to the one used for the cover plate of the film holder was used. A brass block was attached to it so that it could be clamped to the track in the scattering chamber. Two brass bars were bolted to the ring. They were placed horizontally and had slots so that they could be moved in a horizontal direction. To these two bars were bolted two vertical bars. These were also slotted to provide vertical positioning. To the vertical bars was attached the beam stop. With this arrangement the beam stop could be moved both horizontally and vertically.

The best position for the beam stop was found with the use of a gieger counter. Final adjustments were made after exposing several films to determine the exact location of the beam stop with respect to the beam. These exposures ranged from several minutes to 48 hours.

EXPERIMENTAL PROCEDURES

Exposure and Analysis of Films

Eastman Kodak No-Screen x-ray film was cut into strips approximately one by three inches. The lower right hand corner as seen from the x-ray tube was clipped to assure correct orientation when analyzed. The films were all exposed for 48 hours and developed in fresh D-19 developer for

EXPLANATION OF PLATE IV

- Fig. 1. X-ray tube, collimating slits, and scattering chamber.
- Fig. 2. Film holder and beam stop.
- Fig. 3. The third slit and sample holder on front of scattering chamber.

PLATE IV

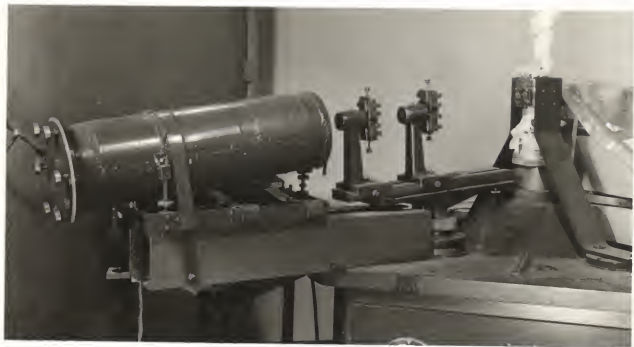


Fig. 1

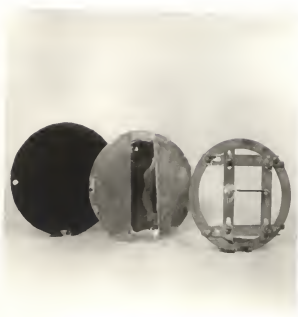


Fig. 2

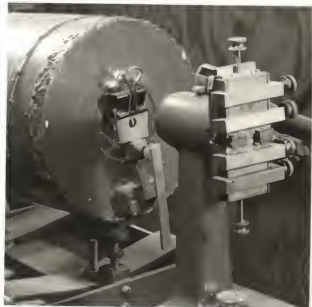


Fig. 3

five minutes. They were then hypoed, washed and dried.

Four scattering pictures and one background picture were made. The four scattering pictures consisted of one using a sample in which the clay particles were randomly oriented and three pictures using samples in which the clay particles had a preferred orientation. For one picture the particles were oriented so that the incident beam was perpendicular to the flat particles. Two pictures were made with the incident beam parallel to the particles, but with the scattering in a plane parallel to the particles for one and perpendicular to the particles for the other.

The scattering pictures were analyzed with a Leeds and Northrup micro-densitometer. The scanner traveled at a rate of 2 mm/min. and the graph paper on which the density curve was recorded traveled at a rate of 2 in/min. The graph paper had a log scale in one direction and five lines per inch in the other. Intensities were measured at every half line and the background subtracted to obtain the actual scattered intensity.

A step exposure was made to check the linearity of the densitometer and film for a given development time. All exposures were then taken in the linear region, that is, where blackening is proportional to intensity.

Calibration

To calculate the angle through which scattering occurred, it was necessary to determine exactly the distance from the sample to the film. The distance along the film from the center to the point at which the intensity is measured divided by the sample to film distance gives the tangent of the scattering angle. For small angles the tangent of an angle is approximately equal to the angle expressed in radians. It was found that for three

degrees or less the tangent and sine of an angle is equal to the angle to four significant figures. Since all the scattering was through angles of less than three degrees, the tangent of the angle was replaced by the angle.

According to Bragg's law, $\lambda = 2d \sin \theta$, a crystal with a large d spacing will produce diffraction lines at small angles. In this case $\sin \theta$ can be replaced by θ so that Bragg's law then reads

$$\lambda = 2d\theta = \frac{ds}{2D}$$

$$\text{or } D = \frac{ds}{2\lambda}$$

where D is the sample to film distance, s is the distance between the diffraction lines on both sides of the undeviated beam, d is the spacing of the crystal, 2θ is the scattering angle, and λ is the wavelength of the x-ray beam. Lead Caprate which has a spacing of 30.33 \AA , was used as a sample. A diffraction picture was obtained in the small angle scattering apparatus. This was analyzed with a microdensitometer and the distance, s , was found to be 171.8 lines on the graph paper. Using the value, 1.5418 \AA , for λ the angle θ was .05083 radians. The value of D was determined to be 1688.3 lines on the graph paper. Since the distance, D , is used in calculating the angle through which small angle scattering occurs, it was left in units of lines. The distance from the center of the beam to the point at which the intensity was measured could be measured with units of lines and the angle could be calculated directly.

Sample Preparation

The Drybranch, Georgia kaolinite clay sample was ground so that the particle would pass through a 100 mesh sieve. The clay was suspended in distilled water. The suspension was allowed to set for about five minutes to let the large particles and agglomerates settle out. The unsettled suspension was then poured into a large flat bottomed dish and this was allowed to settle for several days so the plate-like particles would settle in layers. Most of the water was then siphoned off and the rest removed by evaporation.

To test the sample for preferred orientation of the clay particles, powder patterns were made using cobalt K α -radiation. With the beam striking the sample perpendicular to the particles no preferred orientation was detected as was expected. With the beam striking the sample parallel to the plane of the particles, definite orientation was detected. The orientation was not perfect, but was satisfactory for this work. The powder patterns are shown in Plate V.

The sample for which the beam was incident parallel to the plane particles was made by cutting a square piece from the oriented clay sample and gluing it to a metal plate in which a circular hole had been cut. The samples for which the beam was incident parallel to the plane of the particles were made by slicing the oriented clay sample and then stacking these slices one on top of the other. They were then glued to a holder similar to the one used for the other sample, a metal plate in which a circular hole had been cut. The glue used was 2 per cent parlodion dissolved in amyl acetate.

The samples were not of optimum thickness due to the difficulty in preparing them. The optimum thickness was calculated and found to be .26 mm.

EXPLANATION OF PLATE V

Fig. 1. Powder pattern of oriented sample with beam incident perpendicular to the plane of the particles.

Fig. 2. Powder pattern of oriented sample with beam incident parallel to the plane of the particles. Definite orientation of the particles is indicated.

PLATE V



Fig. 1



Fig. 2

The randomly oriented sample was made this thickness by packing the clay powder into a hole in a piece of metal of this thickness. The sample for which the beam was incident perpendicular to the particles was .36 mm. thick and the sample for which the beam was incident parallel to the particles was .64 mm. thick.

DISCUSSION OF RESULTS

The scattering pictures are shown in Plate VI. These pictures were analyzed with the recording microdensitometer. From the densitometer curves, $\ln I$ and k^2 were calculated. They were plotted with k^2 as the abscissa and $\ln I$ as the ordinate. The resulting curves are shown in Plate VII. The equation of the curve associated with scattering in the plane parallel to the plane of the particle, as indicated by curve A, is independent of the thickness of the particle. The negative slope of this curve is given by equation (11) as $0.272 R^2$ where R is expressed in Angstrom units.

The slopes were measured for two regions on the curve to get a range of values for R . The larger slope was 3130 \AA^2 , and the smaller was 1350 \AA^2 . The radius found using the larger slope was 119 \AA . The smaller radius was 78 \AA .

As a comparison, the range of particle sizes as indicated by the electron micrographs shown in Plate I was measured. The particles ranged in diameter from 2000 \AA to $10,000 \text{ \AA}$. A pseudo radii, then, varied from 1000 \AA to 5000 \AA . The measured thickness of the particles was about 500 \AA .

The particle sizes found by small angle diffraction scattering measurements are clearly too small. The scattering angles for particles larger than 2000 \AA in diameter should be very small and it is most probable that

EXPLANATION OF PLATE VI

Scattering from oriented and random kaolinite particles

Fig. 1. Particles randomly oriented.

Fig. 2. Beam incident perpendicular to plane of particles.

Fig. 3. Beam incident parallel to plane of particles,
scattering perpendicular to plane of particles.

Fig. 4. Beam incident parallel to plane of particles,
scattering parallel to plane of particles.

PLATE VI



Fig. 1



Fig. 2



Fig. 3



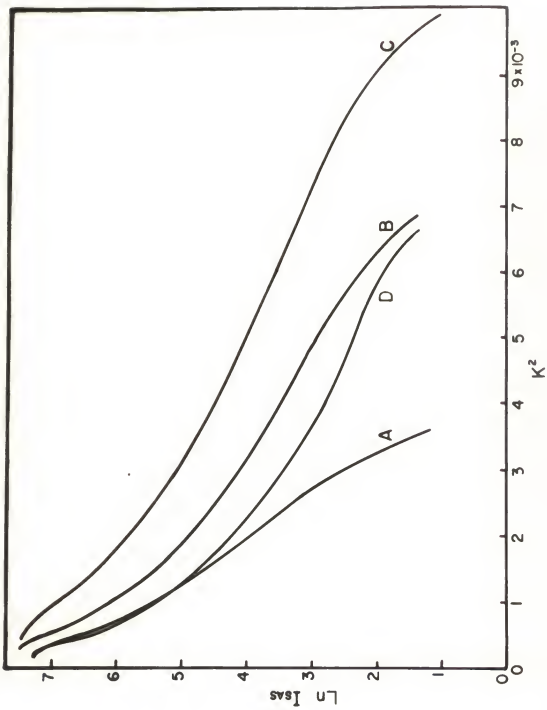
Fig. 4

EXPLANATION OF PLATE VII

Curves showing the natural log of the scattered intensity as a function
of k^2 where $k = \frac{4\pi}{\lambda} \sin \theta$ for various particle orientations.

- Curve A. Beam incident parallel to plane of particles,
scattering parallel to plane of particles.
- Curve B. Beam incident perpendicular to plane of particles.
- Curve C. Beam incident parallel to plane of particles,
scattering perpendicular to plane of particles.
- Curve D. Randomly oriented particles.

PLATE VII



the scattered intensity would lie in the area guarded by the beam stop. The thickness of the kaolinite particles is of the correct order of magnitude for small angle scattering and some scattering should be observed due to the small thickness of the particles. However, the scattering is independent of the thickness when the scattering angle is in the plane of the particle. The conclusion was that the scattering in this case was due to refraction and total reflection.

The scattered intensity due to refraction and reflection from spherical particles is given by Dragsdorff (2) as

$$I = \exp \left\{ \frac{-\lambda^2 k^2}{8\pi \left[\omega_0^2 + \frac{6VD}{R} \delta^2 (\gamma_2 + \ln \frac{\gamma_2}{\delta}) \right]} \right\} \quad (15)$$

where ω_0 is the width at half the maximum intensity of the undeviated beam, V is the specific volume of the sample, D is the thickness of the sample, and δ is given by $1 - \mu$, where μ is the index of refraction. In this work, ω_0 was small and could be neglected.

If $\ln I$ is plotted as a function of k^2 the negative slope of the resulting curve will be given by

$$m = \frac{\lambda^2 R}{48\pi^2 V D \delta^2 (\gamma_2 + \ln \frac{\gamma_2}{\delta})}$$

The radius of the particle can then be found as a function of the slope:

$$R = \frac{4\delta}{\lambda^2 \pi^2 m V D \delta^2 (\gamma_2 + \ln \frac{\gamma_2}{\delta})} \quad (16)$$

Using equation (16) a range of particle sizes was found using the slopes obtained from the curve associated with scattering from the randomly

oriented sample and from the curve associated with the oriented sample with the scattering in the plane of the particle. The two slopes obtained from curve D, the curve associated with the random sample, were 3130 \AA^2 and 420 \AA^2 . The radii found using these slopes were 1796 \AA for the larger slope and 235 \AA for the smaller slope. From curve A, the curve associated with scattering from particles oriented so that the scattering angle was in the plane of particle, the slopes, 3130 \AA^2 and 1350 \AA^2 , were found. The particle radii associated with these slopes were 1306 \AA for the larger slope and 555 \AA for the smaller slope.

The larger particle sizes as determined by the refraction theory fall within the range of particles sizes indicated by the electron micrographs. The smaller radii may be indicative of the thickness of the particles.

It is likely that there is some diffraction scattering due to the thickness of the plate. This dimension is of the correct order of magnitude for small angle diffraction scattering to be observed in our apparatus. The refraction theory gives results more nearly that of the proper order of magnitude. The refracted beam from the larger particles in the sample may have been scattered through angles too small to be measured. This would explain why the largest radius obtained was that of the smaller particles present. This depends, of course, on the relative abundance of small to large particles in our sample.

CONCLUSIONS

The refraction theory based on scattering from spherical particles explains as well as one might hope the scattering from the disc-like kaolinite particles. It is possible that this refraction scattering theory

will give an indication of the thickness of the particles, although it is more likely that the scattering due to thickness will be explained by the diffraction theory.

In a random orientation the scattering from the assumed circular plates should, on the average, be nearly the same as that from spherical particles having the same radius as that of the discs. The refraction and reflection theory certainly has to be modified for any orientation of the particles. This is yet to be done.

The innovation of a field, either gravitational, electric or magnetic to orient the particles for these studies is new. As has been discussed, it is evident that three size parameters and thus a shape should result from such orientations.

SUGGESTIONS FOR FUTURE STUDIES

To complete the problem of resolving the relation of small angle scattering to the sizes of the kaolinite particles, it would be helpful to separate the clay particles into several size ranges. By centrifuging, the particles could be separated into four size groups. One group would consist of particles whose diameters are greater than 2 microns. The second group would have diameters in the range 2 to 0.2 microns. The third group would have diameters of 0.2 to 0.06 microns. The fourth group would contain all the particles whose diameters are less than 0.06 microns. In making this separation the relative concentration of the sample with respect to particle size will be determined. The thickness of these particles will be approximately constant. At least the thickness will not vary over the range that the radii do.

If samples are prepared in the same manner as those used in this work and scattering pictures made and analyzed, there will result 16 curves. From these curves it should be possible to determine how much scattering is due to the thickness of the particles and how much is due to the radii. The scattering associated with the radii should vary with the four samples, but that due to the thickness should remain approximately constant. This will also serve as a check of the interpretation made on the scattering in this thesis. Work on this is underway at the present time.



ACKNOWLEDGMENT

The author gratefully acknowledges the sincere interest and guidance given by Professor R. D. Dragsdorf of the Department of Physics.

LITERATURE CITED

- (1) Boldman, O. E. A., and R. S. Bear.
Effective use of collimating apertures in small-angle x-ray diffraction cameras. *J. App. Phys.* 20, 983-992, 1949.
- (2) Dragsdorf, R. D.
Small angle x-ray scattering. *J. App. Phys.* 27, 620-626, 1956.
- (3) Guinier, A.
Small angle x-ray diffraction. *Ann. Phys.* 12, 161, 1939.
- (4) _____, C. Fournet, C. B. Walker, and K. L. Udowitch.
Small-angle scattering of x-rays. New York: J. Wiley and Sons, Inc., 1955.
- (5) Slack, C. M.
The refraction of x-rays in prisms of various materials. *Phys. Rev.* 27, 691, 1926.
- (6) Von Hardroff, R.
Refraction of x-rays by small particles. *Phys. Rev.* 28, 240-246, 1926.

SMALL ANGLE X-RAY SCATTERING
FROM THIN PLATES

by

RALPH WAYNE DELTREME

B. S., Kansas State College
of Agriculture and Applied Science, 1955

AN ABSTRACT OF A THESIS

submitted in partial fulfillment of the

requirements for the degree

MASTER OF SCIENCE

Department of Physics

KANSAS STATE COLLEGE
OF AGRICULTURE AND APPLIED SCIENCE

1956

The purpose of this work was to develop a method of measuring the sizes and shapes of non-spherical colloidal-sized particles. To test the theory developed, the size parameters of the particles of a common soil clay mineral, kaolinite, were measured. The kaolinite particles are pseudo hexagonal plates. They were approximated as circular discs.

When an x-ray beam impinges upon a particle of constant electron density, the beam is scattered through an angle which depends upon the size, shape and orientation of particles with respect to the incident beam. The scattering angle for colloidal-sized particles is usually less than three degrees.

The intensity of the scattered beam was theoretically determined as a function of the particle size and scattering angle for various orientations of these thin plate-like particles. These intensity equations were rather complicated and so were approximated by Gaussian functions. The natural log of the intensity was plotted as a function of the scattering angle. The slope of this curve was B^2R^2 where B is a constant and R is the radius of the particles.

The samples were made by allowing a suspension of the kaolinite particles to settle in layers. Two samples were made from the oriented clay particles. One would allow the beam to strike the particles perpendicular to the plane of the particles and the other would allow the beam to be incident parallel to the plane of the particles. With the latter two directions of scattering could be observed. One scattering direction would be parallel the plane of the disc and the other perpendicular the plane of the disc.

A copper target x-ray tube was used. The beam was monochromated by use of a nickel filter. A three slit collimating system was used. The detector used by Eastman No-Screen X-Ray film placed in an evacuated scattering chamber.

The particle sizes as determined experimentally using the equations developed for diffraction scattering from circular discs did not agree with the values obtained from the electron micrographs. It was found that diffraction scattering from particles of this size would fall within the area guarded by the beam stop. It was concluded that the scattering observed was due to refraction and total reflection of the x-ray beam by the particles. The values obtained using a theory based on refraction and reflection from spherical particles agreed more closely with the values obtained from the electron micrographs. A modification of the latter theory to oriented disc-shaped particles and extended experimental work on various size ranges of these same particles is planned.